Synthesis of Well-Defined Block Copolymers Tethered to Polysilsesquioxane Nanoparticles and Their Nanoscale Morphology on Surfaces

Jeffrey Pyun,[†] Krzysztof Matyjaszewski,*[,†]
Tomasz Kowalewski,[†] Daniel Savin,[†] Gary Patterson,[†]
Guido Kickelbick,[‡] and Nicola Huesing[‡]

Department of Chemistry, Carnegie Mellon University
4400 Fifth Avenue, Pittsburgh, Pennsylvania 15213
Technische Universität Wien
Getreidemarkt 9/153, A-1060 Wien

Received January 29, 2001

The synthesis of nanostructured organic/inorganic hybrid materials is an area of increasing research activity due to the beneficial synergism of properties these materials possess.[1] An interesting approach to prepare these materials has been the growth of tethered (co)polymers from flat and curved surfaces.[2] A special class of organic/inorganic hybrids is nanoparticles with the polymer chains that encapsulate or are tethered[3] to colloidal materials. A variety of techniques have been developed to prepare inorganic colloids.[4] In the synthesis of hybrid organic/inorganic nanoparticles, these techniques can be applied where the properties of these hybrids can be tuned by introducing functionality to the composition of either the polymeric component or the particle. Modification of the particle composition has been elegantly demonstrated in the synthesis of hybrid silica particles with tethered polystyrene chains.[5]

Herein, we report the synthesis of functional nanoparticles, followed by their use as initiators in atom transfer radical polymerization (ATRP)[6] to prepare hybrid organic/inorganic nanoparticles. In contrast to previous reports, we have focused on the synthesis of core−shell nanostructures via the covalent attachment of block copolymers to inorganic nanoparticles. While various techniques have been reported to synthesize core−shell colloids,[4b] the use of controlled/living polymerization processes to prepare hybrid nanoparticles is a versatile approach enabling the engineering of particle properties by controlling composition and molar mass of the tethered block copolymer. Atomic force microscopy (AFM) studies of these materials revealed the direct impact of the tethered copolymer composition on the nanoscale morphology of hybrid nanoparticle (sub)monolayer films. In particular, the use of AFM was advantageous as both the morphology and volume of hybrid nanoparticles could be determined, as opposed to transmission electron microscopy (TEM) where only two-dimensional information of ultrathin films could be obtained.

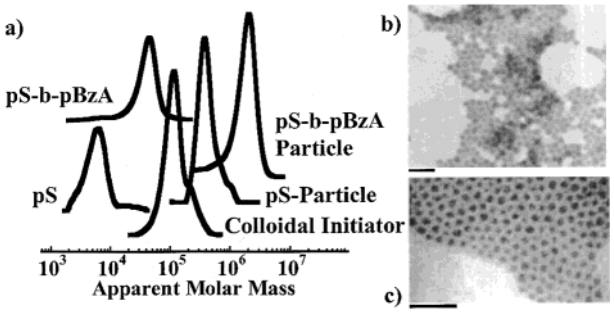

Figure 1. (a) SEC of **Colloidal Initiator**; **pS-grafted particles** prepared by ATRP using $[S]_o = 8.68$ M; $[Br]_o = 0.017$ M; $[Cu(I)Br]_o = 0.008$ M; [dNbpy] = 0.017 M at 90 °C; monomer conversion = 5% (^{1}H NMR); **pS-*b*-pBzA grafted particles** made using $[BzA]_o = 6.18$ M; $[Br]_o = 0.008$ M; $[Cu(I)Br]_o = 0.061$M; $[Cu(II)Br_2]_o = 0.002$ M; [dNbpy] = 0.127 M at 80 °C, monomer conversion = 5% (^{1}H NMR); cleaved **pS homopolymer** $M_{n\ SEC} = 5230$; $M_w/M_n = 1.22$; cleaved **pS-*b*-BzA copolymer** $M_{n\ SEC} = 27280$; $M_w/M_n = 1.48$). (b) TEM image of polysilsesquioxane colloidal initiators. (c) TEM image of pS hybrid nanoparticles ($M_{n\ pS} = 5230$; $M_w/M_n = 1.22$) Black bar = 100 nm.

Scheme 1. Synthesis of 2-Bromoisobutyrate Functional Nanoparticles and pS-*b*-pBzA Hybrid Particles Using Microemulsion and ATRP Processes

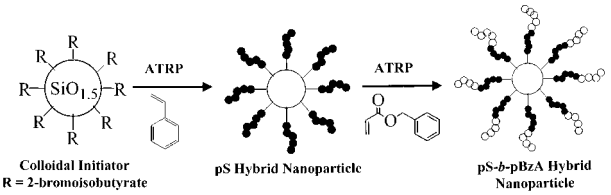

In the preparation of colloidal initiators, 2-bromoisobutyrate (BiB) groups were bound to the colloid to ensure efficient initiation of styrenes and (meth)acrylates by ATRP.[7] In the synthesis, a modified microemulsion process[8] was employed resulting in polysilsesquioxane ($SiO_{1.5}$)[9] nanoparticles (Scheme 1). Elemental analysis of BiB functional nanoparticles indicated that ATRP-initiating groups were incorporated ([Br] = 0.36 mmol/g of particle, 2.9 wt %). Dynamic light scattering (DLS), TEM and AFM of the BiB functional colloids confirmed that discrete particles with nearly uniform effective diameters (D_{eff}) were prepared ($D_{eff\ DLS} = 27$ nm, $D_{eff\ TEM} = 18 + 2$ nm,[10] $D_{eff\ AFM} = 19 \pm 1$ nm.[11] The reasonable agreement of particle sizes obtained from AFM, TEM, and DLS also confirmed proper calibration of AFM measurements.

Size-exclusion chromatography (SEC) of colloidal initiators and hybrid nanoparticles assayed the grafting of (co)polymers by monitoring hydrodynamic volume differences of colloidal initiators and hybrid nanoparticles (Figure 1a). SEC of colloidal initiator revealed a narrow molecular weight distribution, indicative of discrete particles with relatively uniform size. Although molar masses using SEC against linear pS standards were inaccurate due to the higher density of the nanoparticles, SEC enabled facile determination of increases in hydrodynamic volume after the grafting of (co)polymers to the colloidal initiators. SEC traces

[†] Carnegie Mellon University.
[‡] Technische Universität Wien.

(1) (a) Novak, B. M. *Adv. Mater.* **1993**, *5*, 422. (b) MacLachlan, M. J.; Manners, I.; Ozin, G. A. *Adv. Mater.* **2000**, *12*, 675.
(2) (a) Prucker, O.; Ruhe, J. *Langmuir* **1998**, *14*, 6893. (b) Huang, X.; Doneski, L. J.; Wirth, M. J. *Anal. Chem.* **1998**, *70*, 4023. (c) Husseman, M.; Malmstrom, E. E.; McNamara, M.; Mate, M.; Mecerreyes, D.; Benoit, D. G.; Hedrick, J. L.; Mansky, P.; Huang, E.; Russel, T. P.; Hawker, C. J. *Macromolecules* **1999**, *32*, 1424. (d) Matyjaszewski, K.; Miller, P. J.; Shukla, N.; Immaraporn, B.; Gelman, A.; Luokala, B. B.; Siclovan, T. M.; Kickelbick, G.; Vallant, T.; Hoffman, H.; Pakula, T. *Macromolecules* **1999**, *32*, 8716. (e) Zhao, B.; Brittain, W. J. *J. Am. Chem. Soc.* **1999**, *121*, 3557.
(3) (a) Barthet, C.; Hickey, A. J.; Cairns, D. B.; Armes, S. P. *Adv. Mater.* **1999**, *11*, 408. (b) Auroy, P.; Auvray, L.; Leger, L. *J. Colloid. Interface Sci.* **1992**, *150*, 187. (c) Asher, S. A.; Holtz, J.; Liu, L.; Wu, Z. *J. Am. Chem. Soc.* **1994**, *116*, 4997.
(4) (a) Stober, W.; Fink, A.; Bohn, E. *J. Colloid Interface Sci.* **1968**, *26*, 62−69. (b) Caruso, F. *Adv. Mater. (Weinheim, Ger.)* **2001**, *13*, 11.
(5) von Werne, T.; Patten, T. E. *J. Am. Chem. Soc.* **1999**, *121*, 7409.
(6) (a) Wang, J. S.; Matyjaszewski, K. *J. Am. Chem. Soc.* **1995**, *117*, 5614. (b) Patten, T. E.; Xia, J.; Abernathy, T.; Matyjaszewski, K. *Science* **1996**, *272*, 866.
(7) Matyjaszewski, K.; Wang, J. L.; Grimaud, T.; Shipp, D. *Macromolecules* **1998**, *31*, 1527.
(8) Baumann, F.; Deubzer, B.; Geck, M.; Dauth, J.; Schmidt, M. *Adv. Mater* **1997**, *9*, 955.
(9) Zhang, C.; Babonneau, F.; Bonhomme, C.; Laine, R. M.; Soles, C. L.; Hristov, H. A.; Yee, A. F. *J. Am. Chem. Soc.* **1998**, *120*, 8380.
(10) The reader is directed to the Supporting Information for details on TEM images of particles and the calculation of tethered chains per particle from AFM analysis.
(11) The ±1 nm error was not a standard deviation of particle sizes, but an indicator of the accuracy of the AFM measurement. The reader is directed to the Supporting Information for details.

10.1021/ja010241m CCC: $20.00
Published on Web 08/30/2001

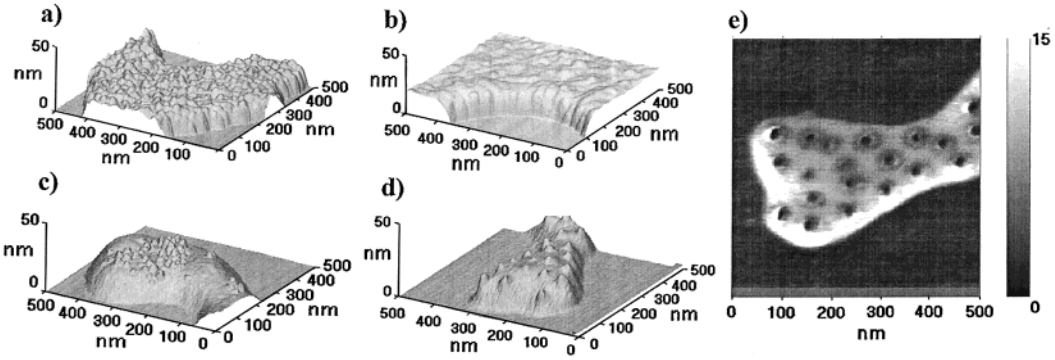

Figure 2. Tapping mode AFM images of nanoparticle (sub)monolayers on mica: (a) colloidal initiators, (b) pS-tethered particles, (c) colloidal initiators blended with untethered pS (M_n = 10,000) (2:1 by wt. of pS to colloid), (d) pS-*b*-pBzA) tethered particles. (e) phase image of a submonolayer patch of pS-*b*-pBzA hybrid particles shown in (d); regions of different phase contrast were identified tentatively as: particle cores (dark spots), pS segment shells (dark halos around particles), pBzA segment (brighter matrix).

of BiB functional particles shifted to higher apparent molar mass after the ATRP of styrene. Further use of the pS hybrid nanoparticle as a macroinitiator for the ATRP of benzyl acrylate (BzA), yielded a pS-*b*-pBzA block copolymer hybrid particle, as evidenced by an additional increase in apparent molar mass.

To verify the successful synthesis of homo- and block (co)-polymers by initiation from the nanoparticles, colloids were destroyed by treatment with hydrofluoric acid (HF), and the remaining (co)polymers were characterized by SEC (Figure 1). The molar mass increase of pS (M_n = 5,230; M_w/M_n = 1.22) and pS-*b*-pBzA (M_n = 27,280; M_w/M_n = 1.48) recovered after hydrolysis of the core also indicated the successful consecutive ATRP of S and BzA from the colloidal initiator. The increase in polydispersity of the cleaved pS-*b*-pBzA copolymer was due to the presence of terminated pS chains formed in the polymerizations ($M_{n\ \mathrm{main\ peak}}$ = 34,810; M_w/M_n = 1.22).

DLS confirmed the grafting of pS ($D_{\mathrm{eff\ DLS}}$ = 52 nm) and pS-*b*-pBzA ($D_{\mathrm{eff\ DLS}}$ = 106 nm) to the nanoparticle initiator and a progressive increase in the D_{eff} after each ATRP reaction.

To obtain particle sizes in the solid state, TEM of $SiO_{1.5}$ colloidal initiators, pS and pS-*b*-pBzA hybrid nanoparticles was conducted. TEM confirmed an increase of D_{eff} from colloidal initiators ($D_{\mathrm{eff}} = 18 \pm 2$ nm, Figure 1b) to pS hybrid nanoparticles ($M_{n\ \mathrm{pS}}$ = 5,230; $D_{\mathrm{eff}} = 27 \pm 2$ nm, Figure 1c) and to higher molar mass pS hybrid nanoparticles ($M_{n\ \mathrm{pS}}$ = 9,850; $D_{\mathrm{eff}} = 31 \pm 2$ nm).[24] However, particle sizes for the pS-*b*-pBzA hybrid nanoparticle ($M_{n\ \mathrm{pS}-b-\mathrm{pBzA}}$ = 27,280) were significantly lower than expected ($D_{\mathrm{eff}} = 29 \pm 2$ nm). The discrepancy in the D_{eff} of the pS-*b*-pBzA hybrid nanoparticle was attributed to the different spreading behavior of tethered pS and pBzA segments on the surface of TEM sample grid. Thus, the particle size of the pS-*b*-pBzA hybrid nanoparticles may have been underestimated using TEM, as the $D_{\mathrm{eff\ TEM}}$ determination relied on two-dimensional area information of the submonolayer patches.[10] To determine accurate particle sizes, volume measurements of hybrid nanoparticle (sub)monolayers were conducted using AFM.

Tapping mode AFM measurements first verified the successful grafting of polymers to nanoparticles and morphology changes of (sub)monolayers of particles on mica after each ATRP reaction (Figure 2). The D_{eff} from AFM images were ascertained from the measured volumes of the colloidal initiator ($D_{\mathrm{eff\ AFM}} = 19 \pm 1$ nm, Figure 2a) pS ($M_{n\ \mathrm{pS}}$ = 5,230; $D_{\mathrm{eff\ AFM}} = 27 \pm 1.5$ nm, Figure 2b) and pS-*b*-pBzA ($D_{\mathrm{eff\ AFM}} = 56 \pm 3$ nm, Figure 2d, e) hybrid nanoparticles. The number of tethered polymers per particle (N_t) was calculated by plotting the apparent volume (V_{app}, obtained from AFM) of colloidal initiators, pS and pS-*b*-pBzA hybrid particles versus the number average volume of the cleaved polymer chain ($V_n = M_n/N_a\rho_{\mathrm{polymer}}$, N_a = Avogadro's number) with the slope being equal to N_t. The linear correlation between these variables indicated that N_t remained constant after each ATRP reaction. Depending on the model of particle packing in AFM analysis, this value was estimated to be between 680 $\pm$ 100 and 1250 $\pm$ 40 chains per particle.[10]

Ultrathin films of (hybrid) nanoparticles displayed unique features in AFM tapping mode images. Bare particles formed tightly packed arrays, with clearly discernible individual nanoparticles. Regular particle arrays were also observed after the ATRP of styrene from the nanoparticle; however, the contours of individual particles were smeared due to the presence of tethered pS chains forming a glassy matrix (Figure 2b). Such smearing of particle contours was not observed in a control experiment, conducted with a (sub)monolayer blend of colloidal initiators and untethered pS standards (M_n = 10000). In contrast, nanoparticle (sub)-monolayers formed tightly packed aggregates surrounded by a matrix of untethered polymer, due to depletion demixing (Figure 2c).[12] Contours of individual nanoparticles were of comparable sharpness as those in experiments with bare particles due to corrugations in the ultrathin film. AFM images of (sub)monolayers formed by pS-*b*-pBzA particles revealed strikingly different features, indicating the successful extension of the pBzA segment from the pS particles (Figure 2b, d). The pS-*b*-pBzA hybrid particles appeared as core−shell spots with distinctly different shells embedded in a continuous phase (Figure 2e) in AFM phase images, mapping the phase shift between the oscillation of the drive and cantilever. Such contrast resulted presumably from the differences in the energy dissipation by the inorganic phase (dark center spots), the glassy pS inner shell (round halos) and the rubbery outer shell of pBzA comprising the matrix.

In conclusion, we have prepared hybrid nanoparticles using ATRP possessing well-defined tethered homopolymers of pS and block copolymers of pS-*b*-pBzA. The ability to use ATRP enables a wide range of functional copolymers to be incorporated onto colloids with the potential to form a variety of layered core−shell structures.

Acknowledgment. We gratefully acknowledge Professor Manfred Schmidt for helpful discussions, and Joseph Suhan (CMU) for TEM analysis of nanoparticles. The NSF (T.K.: DMR 9871874; K.M.: DMR 9871450), the ATRP/CRP Consortia and the Vienna University of Technology (J.P.) are acknowledged for funding.

Note Added after ASAP: In the version posted August 30, 2001, there were typographical errors on the second page, second column. The correct version was posted September 19, 2001.

Supporting Information Available: Experimental details describing the synthesis and characterization of (hybrid) nanoparticles. TEM and AFM images of hybrid nanoparticles, and SEC chromatograms of the cleaved polymers; calculations of the number of tethered chains per particle (PDF). This material is available free of charge via the Internet at http://pubs.acs.org.

JA010241M

(12) Lindenblatt, G.; Schärtl, W.; Pakula, T.; Schmidt, M. *Macromolecules* **2000**, *33*, 9340.